J MATER RES TECHNOL. 2019;8(2):1653–1662

Available online at www.sciencedirect.com

jmr&t Journal of Materials Research and Technology

www.jmrt.com.br

Original Article

Characterization of DLC coatings over nitrided stainless steel with and without nitriding pre-treatment using annealing cycles

Eugenia. L. Dalibón[a,*], *Thierry Czerwiec*[b], *Vladimir J. Trava-Airoldi*[c], *Naureen Ghafoor*[d], *Lina Rogström*[d], *Magnus Odén*[d], *Sonia P. Brühl*[a]

[a] *Surface Engineering Group, Universidad Tecnológica Nacional (UTN-FRCU), Ing. Pereira 676, E3264BTD Concepción del Uruguay, Argentina*

[b] *Institut Jean Lamour UMR 7198, CNRS, Université de Lorraine, Dept. CPSS, 54011 Nancy, France*

[c] *Instituto Nacional de Pesquisas Espaciáis (INPE), Av. dos Astronautas 1758, 12.227-010 São José dos Campos, SP, Brazil*

[d] *Nanostructured Materials, Department of Physics, Chemistry and Biology (IFM), Linköping University, SE-581 83 Linköping, Sweden*

ARTICLE INFO

Article history:
Received 24 June 2018
Accepted 1 December 2018
Available online 12 January 2019

Keywords:
DLC coatings
Thermal stability
Duplex treatment
Nitriding

ABSTRACT

Amorphous hydrogenated diamond-like carbon (DLC) coatings were deposited using plasma assisted chemical vapour deposition (PACVD) on precipitation hardening (PH) stainless steel. Plasma nitriding has been used as pre-treatment to enhance adhesion and mechanical properties. Chemical and mechanical properties of DLC coatings are dependent on the hydrogen content and so on the relation between sp^3/sp^2 bondings. The bondings and the structure of the DLC film change with temperature. In this work, a study of the thermal degradation and the evolution of the mechanical properties of DLC coatings over PH stainless steel have been carried out, including the effect of an additional nitrided layer.

Nitrided and non-nitrided steel samples were subjected to the same coated in the same conditions, and they were submitted to the same thermal cycles, heating from room temperature to 600 °C in several steps.

After each cycle, Raman spectra and surface topography measurements were performed and analyzed. Nanohardness measurements and tribological tests, using a pin-on-disc machine, were carried out to analyze variations in the friction coefficient and the wear resistance.

The duplex sample, with nitriding as pre-treatment showed a better thermal stability. For duplex sample, the coating properties, such as adhesion, and friction coefficient were sustained after annealing at higher temperatures; whereas it was not the case for only coated sample.

* *Corresponding author..*
E-mails: dalibone@frcu.utn.edu.ar (E.L. Dalibón), thierry.czerwiec@univ-lorraine.fr (T. Czerwiec), vladimir@las.inpe.br (V.J. Trava-Airoldi), naugh@ifm.liu.se (N. Ghafoor), linro@ifm.liu.se (L. Rogström), magod@ifm.liu.se (M. Odén), sonia@frcu.utn.edu.ar (S.P. Brühl).
https://doi.org/10.1016/j.jmrt.2018.12.002

1. Introduction

Despite their amorphous characteristics and the presence of hydrogen carbon bondings, diamond-like carbon (DLC) coatings have unique properties similar to diamond such as very high hardness, chemical inertia, and a very low friction coefficient compared to other hard coatings.

DLC coatings can be deposited via plasma-assisted techniques, from a solid carbon target, such as plasma vapour deposition (PVD) or via hydrocarbon precursors by plasma assisted chemical vapour deposition (PACVD). In the latter case, the presence of hydrogen in the film cannot be avoided, and the chemical bondings are not only C—C but also C—H, with different proportions of sp^3 and sp^2 bondings, depending on plasma deposition parameters such as time, temperature and gas flow [1–3]. In a wide range of structures, these films have properties similar to diamond such as high hardness, a very smooth surface with a low coefficient of friction (below 0.1) and very good wear and corrosion protection properties. However, these properties are not only affected by film structure but also by the tribosystem properties: hardness profile, adhesion, mechanical support and stresses. For these reasons nitriding has been used as pre-treatment, especially over soft substrates such as stainless steel [4–6].

Duplex treatments combining nitriding and DLC coatings can be used to increase the mechanical properties and tribological performance by increasing the load bearing capacity of the so-formed composite. Such duplex treatments with nitriding are often applied on medium alloy steels as substrates [7,8]. It was reported that a good wear resistance was obtained with the DLC deposited over a hard and homogeneous compound layer [8,9]. Although other authors found that the best load-bearing capacity was achieved for a nitrided layer primarily constituted by a diffusion layer [7].

In the case of stainless steels, where only a nitrogen-expanded phase arises after low temperature nitriding, some papers were previously published [10–12].

DLC coatings are frequently used in applications for which there may be high work temperature or localized heating caused by friction. Hence detailed studies of the evolution of coating properties with thermal solicitations are necessary, for example, to use it in engine components [13,14]. Several studies about the thermal stability of DLC were found in the literature, reporting detrimental structural changes caused by the change in the carbon bondings, from sp^3 to sp^2 [15,16]. Also, some papers were published about improving thermal stability using dopant elements or nanoparticles incorporated to the film [17–19].

A preliminary work was published on the thermal behaviour of duplex coatings [20]. In this work a different thermal degradation between duplex and coated samples was detected. The nitriding treatment improved not only the adhesion of the coating but it also affected the surface properties. It was decided to continue with the research in this topic, analyzing new aspects. The main goal of the present work is to study not only changes in structural properties but also the tribological behaviour of DLC coatings deposited on nitrided and non-nitrided precipitation hardening (PH) stainless steels going further than in the previous work. Raman spectra were performed, and a complete study of the film properties and degradation after the different annealing cycles was carried out. Topography measurements were performed to improve the understanding of the coating degradation and friction coefficients measurements are presented. The influence of the nitrided layer on the thermal behaviour of the DLC coating is analyzed.

2. Experimental

PH martensitic stainless steels (Corrax® from Uddeholm) were used as base material. The chemical composition in weight percentage of Corrax® is 0.03% C, 12% Cr, 1.4% Mo, 0.3% Mn, 0.3% Si, 9.2% Ni, 1.6% Al and Fe as balance.

Disc-shaped samples were cut from a 25 mm in diameter bar and they were hardened by means of an ageing process for two hours at 530 °C according to supplier recommendations. One group of samples was nitrided in an industrial reactor using a DC pulse discharge at 390 °C for 10 h in a 25% N_2 + 75% H_2 gas mixture.

DLC coatings were deposited on all samples by PACVD using methane as gas precursor. The process total gas pressure was of 10 Pa at 10 ml/min gas flow during 2 h. Structural properties of the nitrided layer and the DLC film without annealing, so as the duplex system and corrosion properties have been published before [10,11,21,22]. The group, which was not nitrided, but with a deposited coating was named “coated samples” and the one, which was previously nitrided, was named “duplex samples”. The coating thickness was about $3.0 \pm 0.3\,\mu m$ with a silicon interlayer of $0.3\,\mu m$ and the nitrided layer thickness was of $14 \pm 1\,\mu m$ approximately.

The heat treatment post DLC deposition consisted of annealing steps at 200 °C, 300 °C, 400 °C, 500 °C and 600 °C for 1 h, counting from the time the temperature step was reached. The heating rate was 20 °C/min and both coated and duplex samples were heat treated in a vacuum chamber, following a procedure reported previously in the literature [22]. In each step, one group of samples was taken out. So at the end, five groups of samples annealed at different temperatures were studied, each group with equal quantity of coated and duplex samples.

The DLC coatings were characterized by Raman spectroscopy. The Raman spectra were fitted using two Gaussian lines. The intensity for each band was determined and the I_D/I_G ratio was calculated. The hydrogen content was estimated using the slope of the photoluminescence background in the Raman spectra taking into account the model proposed by Casiraghi et al. [23].

The surface was observed by electronic microscopy and white light interferometry (WLI) using 20× objective. Both surface map and profile were obtained by Metropro© software. Moreover, focused ion beam (FIB) cuttings were performed in different regions of the surface samples in order to observe the cross section and to measure the DLC thickness after the annealing. Mechanical properties were assessed using instrumented nanoindentation with 15 mN load.

Sliding wear tests were carried out using 2 N load, 1800 cycles, 1 mm of amplitude and alumina balls ($\phi = 6$ mm) as counterpart to evaluate the tribological behaviour of the

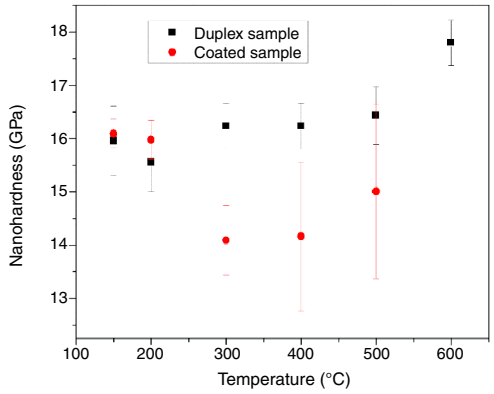

Fig. 1 – Variation of nanohardness in DLC coatings after the annealing cycles at different temperatures for duplex and coated samples.

coatings. Three tests were performed for each sample. The wear tracks were observed by SEM and WLI. After annealing, the degradation of the surface could be evaluated from the values of the coefficient of friction and the observation of the surface damage along and at the sides of the wear tracks. The changes in film properties, surface topography and tribological behaviour were compared after each thermal cycle to describe the coating degradation with temperature.

3. Results

3.1. *Changes in film properties with thermal cycles*

The hardness for the DLC films and for the nitrided layer were 16 ± 1 GPa and 11 ± 1 GPa respectively as it was reported in a previous publication [11]. The mean values for nanohardness measured after each annealing cycle are presented in Fig. 1, comparing coated and duplex samples. Twenty measurements in different places were carried out and the magnitude of the error was the standard deviation of the measured values. As the indenter penetration is less than 10% of the film thickness, this hardness value can be considered as a film property without the influence of the substrate.

In this test, some differences became visible. For the duplex sample, the nanohardness values did not have an appreciable variation, up to 500 °C. Only at 600 °C, some changes were observed, which were probably caused by structural modification.

On the other hand, a hardness decrease was noticed in the coated sample at 300 °C. Probably, a degradation that cannot be observed occurred at the interface between the DLC coating and the substrate. However, no changes were observed neither in surface images nor in the Raman spectrum, as it will be mentioned below.

At higher temperatures, the dispersion increased in the coated sample as it can be observed in Fig. 1. It is pointless to indicate a mean nanohardness value when the annealing was performed at 600 °C because the dispersion is very high. The nanohardness changes from one point to another on the surface sample were between 4 GPa and 14 GPa.

This fact can be explained in two ways. The coating was detached partially or the film suffered a structure or composition change. The first one could be easily observed in some regions of the surface and the second one was analyzed with Raman spectroscopy and the results are presented below. When graphitization occurs in DLC films, the hardness decreases [18].

The Raman spectra allowed the possibility to evaluate the film structure. It can be seen in Fig. 2 that both groups of samples presented similar features after annealing at 200 °C and 300 °C. The DLC without thermal post treatment was analyzed as well and it was depicted for comparison in black. In this case, the Raman spectrum presented the classical two overlapping bands D and G, which, as it was already published, were well positioned, in 1379 cm^{-1} and 1554 cm^{-1} [15,16]. However, in the coated sample at 400 °C, it could be noticed that the film transformation started because the characteristic G and D bands of DLC coatings could not be distinguished (Fig. 2). On the other hand, in the duplex sample, this did not occur until reaching a temperature value of 500 °C (Fig. 2).

After annealing at 200 °C and 300 °C, a slight shift in the D and G peak positions was detected, as it is shown in Fig. 2 and Table 1. For these temperatures, in both samples, it was possible to measure the D and G bands position, the intensity ratio between the D and G bands and the D and G bands width, indicating only a very small graphite domain for both samples (see Table 1).

For higher annealing temperatures, it was not possible to perform an accurate analysis of the DLC coatings. A very strong fluorescence appeared at 400 °C, revealing degradation of the structural properties of the film in the case of the coated sample (Fig. 2). On the contrary, in the duplex sample, the analysis of the Raman spectrum corresponding to 400 °C annealing could still be carried out. The degradation starts at 500 °C, as it can be observed in the Raman Spectrum of Fig. 2, where the G and D bands cannot be differentiated. Finally, at 600 °C, there was no characteristic DLC coating structure in the Raman spectrum for both groups of samples.

3.2. *Changes in surface topography and film integrity*

Surface topography did not change after the annealing at 200 °C and 300 °C in both coated and duplex samples. Moreover, this latter did not present changes in the surface topography after the annealing at 400 °C (Fig. 3a). However, different features indicating a film transformation appeared when the surface of the coated samples was observed after the 400 °C cycle. In fact, part of the film was delaminated; bubbles and holes were formed, as it is shown in Fig. 3b. Moreover, the existence of holes was confirmed by the different heights detected on WLI Images (Fig. 4a and b). It should be mentioned that the presence of the coating, even thinner, was confirmed by EDS analysis in all regions of interest (not shown).

In the duplex samples, some changes could be observed on the coating surface at the end of the annealing process at 500 °C, as it is shown in Fig. 5a. This sample presented some cracks on the surface (Fig. 5a) but there was not detachment of the coating in any region. After annealing at 600 °C, the

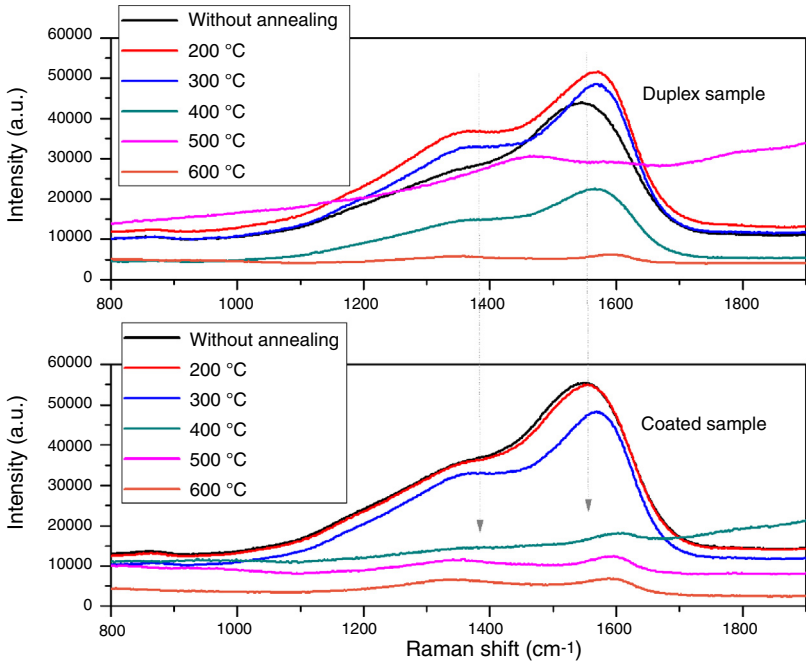

Fig. 2 – Raman spectrum of the duplex and coated samples after annealing at different temperatures.

Table 1 – Analysis of Raman spectra.

Samples	D position	G position	I_D/I_G	D width	G width
Duplex sample without annealing	1379	1554	0.66	283	132
Duplex sample 200 °C	1390	1570	0.88	289	121
Duplex sample 300 °C	1395	1573	0.83	285	104
Duplex sample 400 °C	1388	1570	0.76	276	109
Coated sample without annealing	1383	1557	0.71	283	127
Coated sample 200 °C	1388	1561	0.74	284	121
Coated sample 300 °C	1394	1572	0.83	284	103

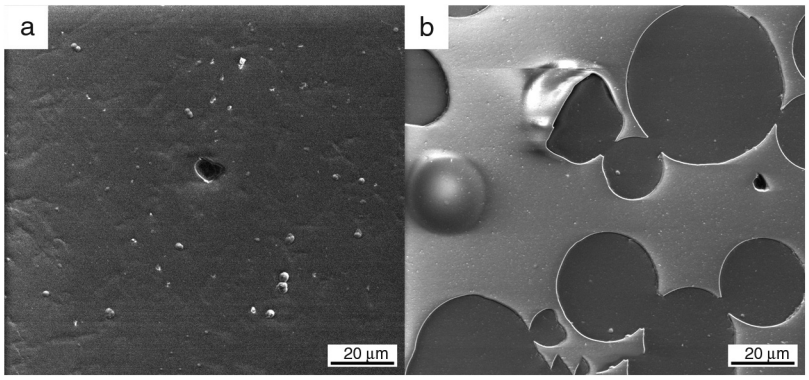

Fig. 3 – SEM image of the samples surfaces after annealing at 400 °C: (a) duplex sample and (b) coated sample.

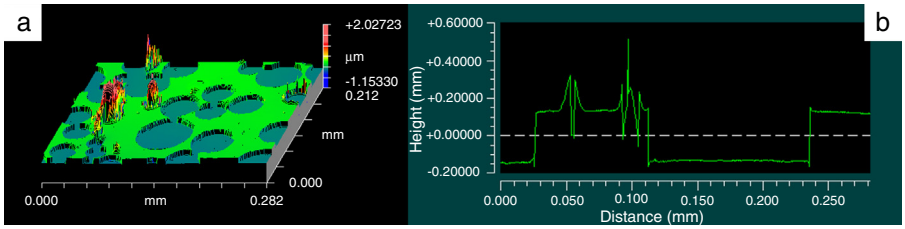

Fig. 4 – (a) WLI image of the coated sample surface after annealing at 400 °C and (b) WLI surface profile.

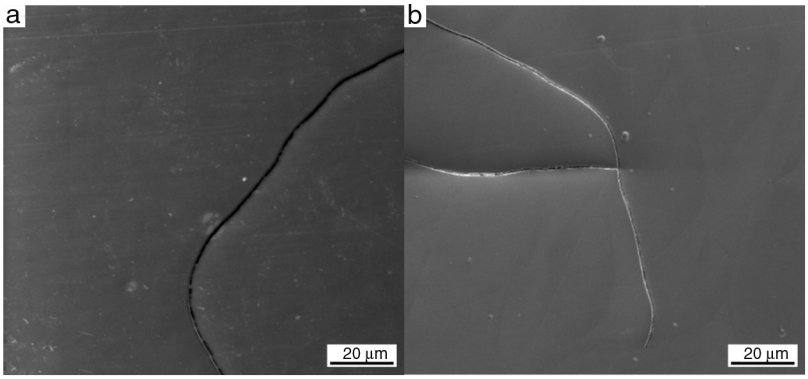

Fig. 5 – SEM image of the duplex sample surfaces after annealing at (a) 500 °C and (b) 600 °C.

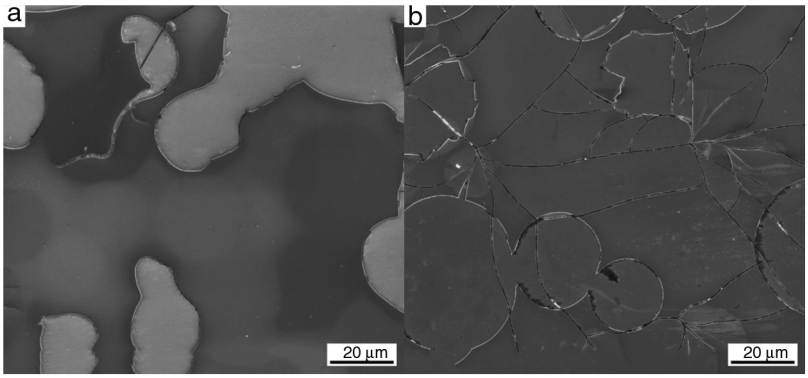

Fig. 6 – SEM image of the coated sample surfaces after annealing at (a) 500 °C and (b) 600 °C.

sample had more cracks as it can be seen in Fig. 5b, indicating a major degradation of the coating. However, the degradation of the duplex coatings is much less than that of the only coated samples.

Indeed, in the coated samples some cracks are observed in regions where the coating was partially detached at the end of the annealing cycle at 500 °C (Fig. 6a). The degradation of the coating was greater after the annealing at 600 °C (Fig. 6b). However, the coating was not completely peeled off but some surface layers were gone.

In the coated sample surface, three FIB cuts were performed and the location is indicated in Fig. 7. The first one covered a region of a hole defect from the outside to the inside (region named 1), the second one, on the edge of a protuberance with a delaminated part (named 2), and the third one, over a protuberance (named 3). In region 1, Fig. 7c, a step can be observed. The right part of the coating has a thickness similar to the original coating, showing that the film has not been damaged there. In the left part of the film, thickness is only 15% less than the right part, showing that the film was not totally removed. In regions 2 and 3, Fig. 7b and d, some delaminated layers of the coating can be observed in the cross section. It can be seen that the minimum film thickness was 1.5 μm, indicating that part of the film was still there but thinner than the not annealed one (2.7 μm). It can be concluded that several layers of the coating were degraded and detached, i.e. the coating delamination occurred by sheets, revealing a cohesive failure.

3.3. *Tribological behaviour*

The evolution of the friction coefficient (μ) is shown in Fig. 8 as a function of time for two annealing temperatures. Other tribological results (final μ values and wear damage) are presented in Table 2 for duplex and coated samples. After annealing at 200 °C and 300 °C, the steady value of μ for both samples was low and similar, about 0.2. This value is in the range of those that have been reported for this kind of coatings in the literature [24]. The presence of the coating strongly reduced the friction coefficient in comparison with steel, with or without the nitrided layer, which is about 0.7. This is due to the formation of a graphite transfer layer which has a self-lubricating effect [24,25]. At 200 °C and 300 °C the track was almost undetectable, indicating that the film was intact. After higher temperature cycles, the wear tracks were visible but very irregular in width and depth. For this reason, a wear volume loss could not be calculated. In addition, the coefficient of friction becomes higher and irregular due to the surface inhomogeneities and areas with different coating thickness and flaking.

The friction coefficient increased for the coated sample after the annealing cycle at 400 °C. It reached values that correspond to the untreated steel friction coefficient (0.8–0.9 in the same test conditions). On the other hand, for the duplex samples, the friction coefficient did not raise that much after annealing at the same temperature; it begins at 0.2 and it reached a final value of 0.47, as it can be observed in Fig. 8.

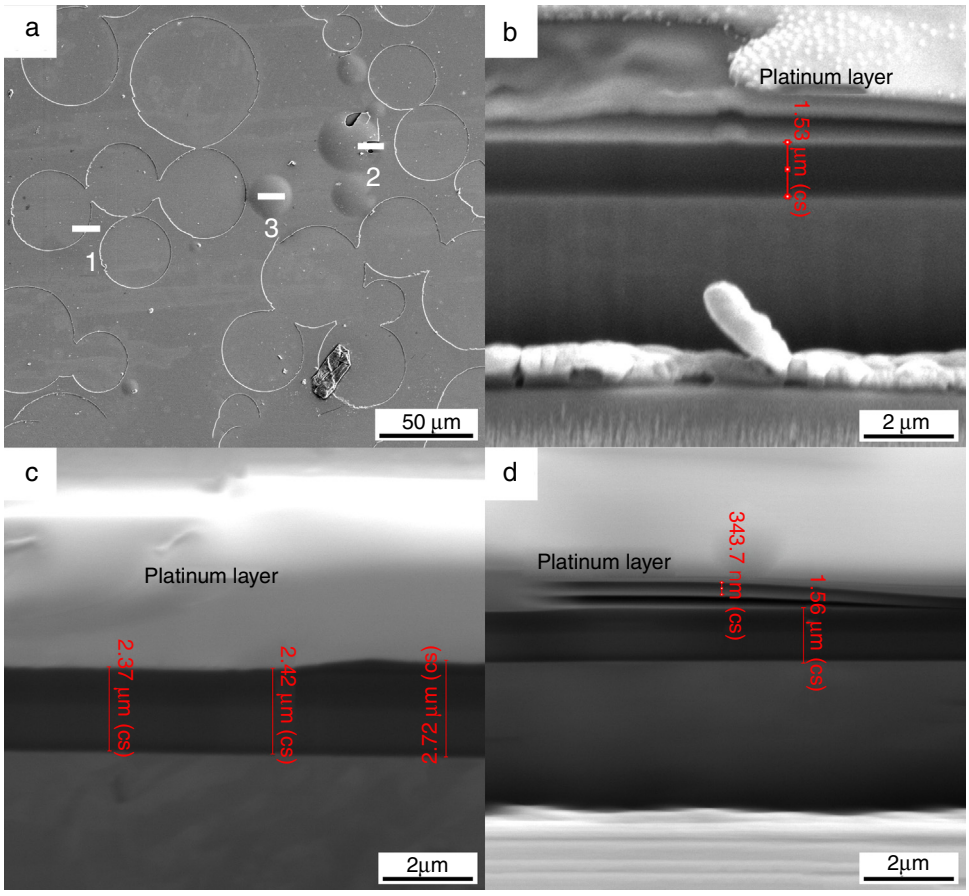

Fig. 7 – (a) SEM image of a surface region, where the film was degraded in the coated sample after annealing at 400 °C, showing the three regions were FIB cuts were performed. (b) Cross section in region 2, a protuberance that was in part peeled off, can be observed. (c) The step in the cross section of region 1. (d) The subsurface structure of a protuberance, corresponding to region 3.

Table 2 – Summary of the tribological results for duplex and coated samples.

Annealing (°C)	Duplex sample		Coated sample	
	μ (steady or final)	Wear damage	μ (steady or final)	Wear damage
200	0.20 ± 0.01	Undetectable track	0.20 ± 0.01	Undetectable track
300	0.20 ± 0.01	Undetectable track	0.20 ± 0.01	Undetectable track
400	0.47 ± 0.08	Detectable track	0.86 ± 0.08	Coating detachment
500	0.77 ± 0.07	Coating detachment	0.90 ± 0.09	Coating detachment. Greater damage than in the duplex sample.
600	0.90 ± 0.09	Coating detachment	0.90 ± 0.09	Coating detachment

After annealing at 600 °C, the friction coefficient rapidly reached the value of the base material for both samples (Table 2), indicating that the coating has detached during the test and the wear damage occurred on the substrate. In fact, the wear track depth was greater than the coating thickness for both samples.

As a summary, the difference in tribological properties between both groups of samples occurred after annealing at 400 °C. The μ values remained rather low after the annealing process only in the duplex samples. It could be confirmed not only that the coating was still present, but also that it has maintained its properties. As it was already mentioned in Section 3.2, the coating is thinner and did not detach completely, some parts of it remained on the surface.

Fig. 9 presents SEM pictures of parts of the wear tracks at the end of the tribological test for annealed samples at 400 °C. A high magnification was selected, with the intention to show topography features within and around the track. In Fig. 9a, which corresponds to the wear track on the coated sample, the coating detachment is clearly visible; in fact, chemical elements corresponding to the steel substrate and aluminium of the counterpart could be detected by the EDX analysis. Moreover, some dark particles were also observed in the track. Since the EDX analysis shows that they are containing oxygen, it

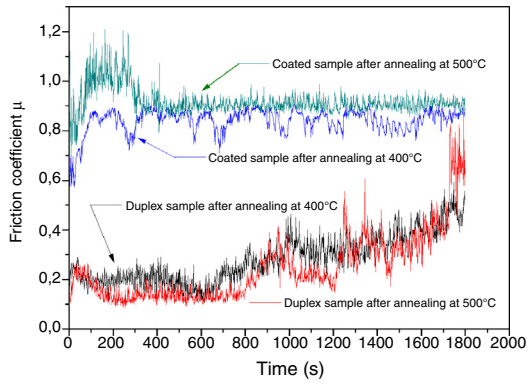

Fig. 8 – Friction coefficient versus time in the wear test for duplex and coated samples annealed at 400 °C and 500 °C.

can be deduced that they are oxidized debris. The mean track width was 380 μm in this case.

In Fig. 9b, which corresponds to the wear track on the duplex sample, only some grooves in the direction of movement and some small damaged regions can be observed. The wear mechanism could be classified as mild abrasive. The coating was still or always present in the wear scar and around it, even in the damaged areas, as it could be confirmed by the EDX spectrum, in which Si and C were detected. With less magnification, the whole scar could be observed, and the mean width was about 150 μm.

At the end of the wear tests on samples after annealing at 500 °C, some flaking could be detected in the wear tracks as it can be seen in Fig. 10a and b. In these figures, only parts of the tracks are presented, because focus was made on the edge of the wear scar to observe the damage features. Outside the track, the film surface can always be observed and it is clear, by comparing both figures, that the damage was already present before the test. It can also be observed that the degradation was more extended in the coated sample than in the duplex one.

Looking inside the wear track in the coated sample (Fig. 10a), adhesive wear clearly occurred, and large plate-like wear debris could be found as other authors also reported [26]. It is well known that bonding occurs between surface asperities, and when these junctions are broken, new ones are formed as large lumps and transfer of materials comes as a result. A large amount of plastic deformation is usually associated with this mechanism [24,26]. The wear was severe in this case; the elements from the substrate and also Al from the counterpart were detected by EDX analysis. On the contrary, in the duplex sample, the damage could be described as mild abrasive wear. Soft grooves with some dark regions, which correspond to oxidized particles, can be observed (Fig. 10b) [27].

4. Discussion

An explanation about the different behaviour of DLC coated PH samples with and without nitriding pre-treatment can be proposed and, related to this point, some hypotheses are described below.

The first one is the chemical modification of the DLC film with an increase in temperature. It is known that DLC films transform to an aromatic ring structure and then to disordered graphitic ring structure during annealing at temperature

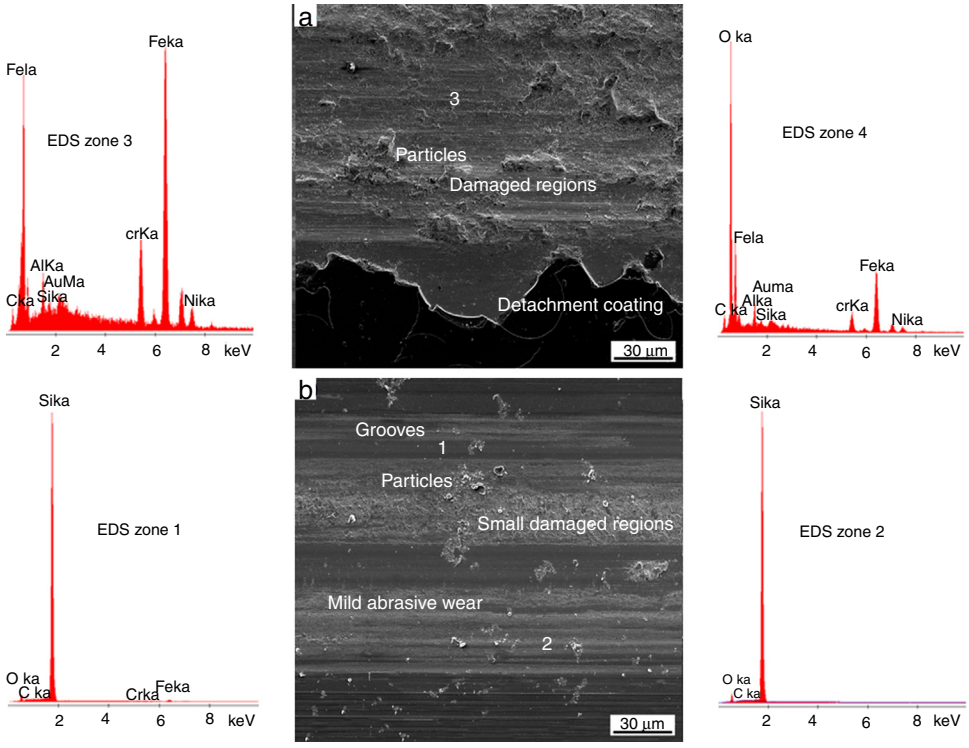

Fig. 9 – SEM images of the wear track and EDX analysis at the end of the tribological test for annealing at 400 °C: (a) duplex sample and (b) coated sample.

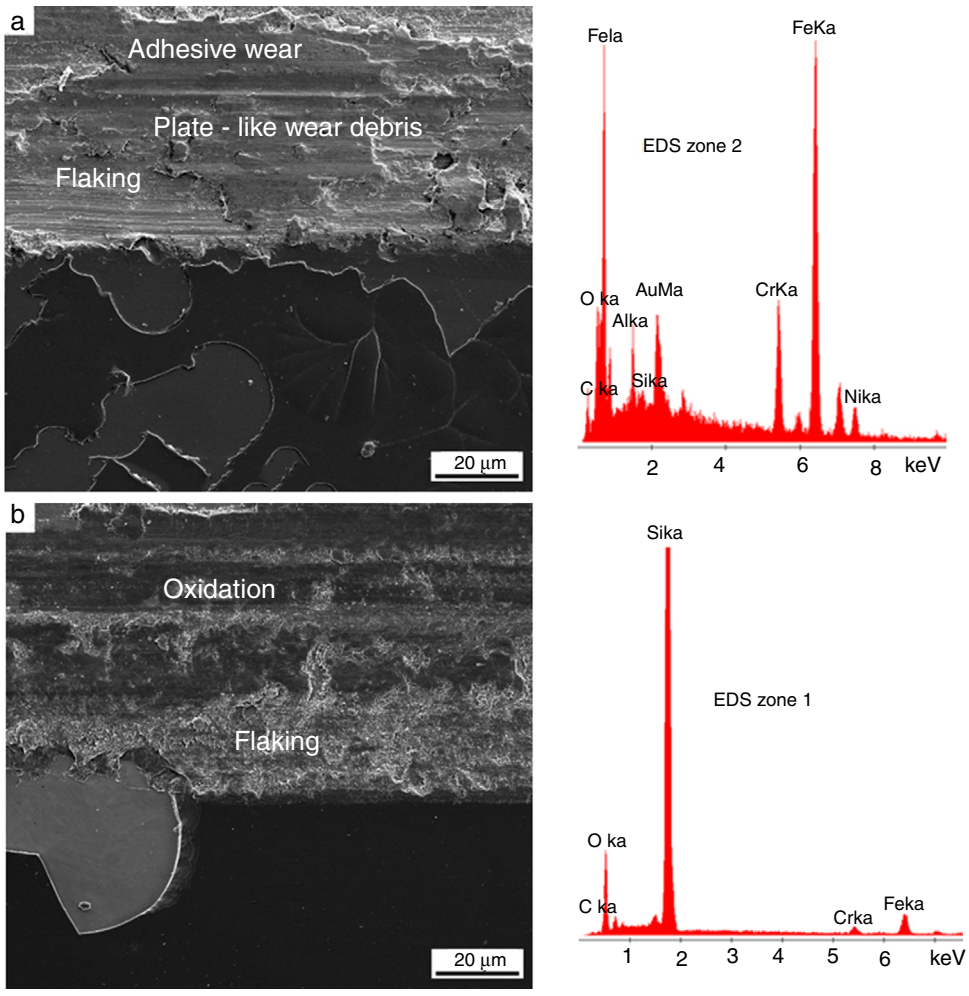

Fig. 10 – SEM images of the wear track and EDX analysis at the end of the tribological test after annealing at 500 °C: (a) duplex sample and (b) coated sample.

higher than 400 °C [28]. With increasing annealing temperature, the structural disorder decreases and the size of graphitic domains increase [28,29].

Such phenomenon is associated with plastic deformation, which reduces the internal stress and in turn the hardness of the DLC coating. According to the results presented above, from properties such as hardness and the observation of surface morphology, it can be stated that the transformation of the DLC coating in graphite was produced at a higher temperature in the duplex sample than in the coated sample. This could be confirmed by the Raman analysis, where the modification and the shift of the classical DLC peaks is a sign of coating degradation. Such degradation was detected in both groups of samples at 600 °C. However, this phenomenon occurred at a higher temperature in the case of the duplex samples as compared to the only coated samples. It is highly probable that in the duplex sample, the rate of graphitization in the coating was lower than in the coated samples. Therefore, the film transformation did not have so much influence on the coating properties and it was also less noticeable. This change in graphitization is probably related to a change in the thermal conductivity as will be discussed later.

The difference between both groups of samples is the nitriding pre-treatment. The influence that it has on the film adhesion, which was better in the duplex sample than in the coated sample, was reported in a previous paper [11]. The nitrided layer raises the load bearing capacity of the system. This layer generates a graded interface between the coating and substrate, increases the hardness of the substrate, reduces the stresses and improves the adhesion as it was published also by other authors [11,30,31]. Moreover, in both samples, a silicon interlayer was deposited previous to the coating. As a result, there is a chemical affinity between this Si layer and the nitrogen of the nitrided layer. So, in the duplex sample, Si reacts with N forming silicon nitride bonds, as pointed out by some of the authors, when XPS analysis were performed in a thin Si layer deposited onto nitrided steel [32,33]. Since hardness and adhesion are higher for the duplex coating, consequently it is more stable at higher temperatures.

Regarding thermal conductivity, the silicon adhesion layer has a thermal coefficient ($3.2 \times 10^{-6}\,K^{-1}$) comparable to those from DLC ($2.3 \times 10^{-6}\,K^{-1}$) and from the nitrided layer ($7.6 \times 10^{-6}\,K^{-1}$) but lower when compared to the one of bare stainless steel ($14.5 \times 10^{-6}\,K^{-1}$). As a consequence, thermal

stress is lower in the duplex sample than in the coated sample [34,35]. On the other hand, the thermal conductivity of DLC is very low; it can be hundred times lower than the thermal conductivity of steel. Therefore, if the adhesion is higher for the duplex coating, the heat dissipation is higher as well and the film resists more to the thermal effect. A thin film without good adhesion due to the low thermal conductivity heats rapidly modifying its structure, i.e. going faster to a structure close to the graphite or to a graphite-like film. As the duration of the thermal cycle is only one hour, a delay can exist before the establishment of a stabilized temperature between nitrided and non-nitrided samples. Thus, some bubbles could be formed in the film with worse adhesion caused by the release of bonded and unbonded hydrogen during the annealing, as it was reported by other authors [34,36]. However, the bubble formation was not observed in well adherent films, e.g. the duplex sample. This could be due to a more efficient heat dissipation.

A relation between nanohardness measures and adhesion can thus be established. That is, whenever a thin film that is well adhered, the hardness measurement is more trustable because the well-adhering film has the substrate as a more efficient support. On the other hand, the non-adherent film is "loose" on the substrate, not allowing the hardness measurement to be real, as well as being closer to the graphite structure. In this work, it was quite clear that the dispersion of the nanohardness measurements in the coated sample observed in Fig. 1 was directly related to the dispersion of the adhesion through the interface, caused by the film degradation.

The friction coefficient remained similar to the DLC coating without thermal treatment after the annealing at 200 °C and 300 °C for both samples. After the annealing at 400 °C, the friction coefficient was low (0.2) at the beginning. After 800 s the value increased for both samples, but at the end it was higher for the coated sample than the duplex sample. Probably as the hardness was lower for the coated sample compared to the duplex sample and the original coating, the penetration of the counterpart was deeper, so the real contact area increased and consequently the friction coefficient too [26,37]. The friction coefficient increased when the annealing temperature was higher. This could be due to the fact that the annealing at high temperatures produces the effusion of hydrogen and deteriorate the coatings tribological properties, as it was reported in the literature [38]. Moreover, the coating properties (hardness, topography and thickness) effectively changed after the annealing at this temperature, as it was presented in the previous sections. Consequently, the mechanical resistance of the system decreased and the wear mechanisms changed. It is clear that the wear damage became greater with the increasing annealing temperature but, in all cases, the damage was worse in the coated sample than in the duplex one.

5. Summary and conclusions

As a summary of results, it can be stated that at the same temperature, the coating degradation is always lower in the duplex sample than in the only coated one. Moreover, the degradation or the morphology changes are different in the two groups of samples. In the duplex, cracks appear on the film surface and no delamination was observed, meanwhile in the coated sample, the film has cohesive failures and it detached layer by layer. Changes in structure properties appear at 400 °C in the coated sample and at 500 °C in the duplex one.

It was shown that the low friction coefficient and good tribological properties of the DLC coating remained unchanged in the duplex samples after an annealing process at 400 °C. It was also observed that the nanohardness values did not decrease after thermal treatments, even at high temperatures.

It was proved that a nitriding treatment previous to the coating deposition improves the DLC thermal stability through the thermal annealing cycles, if compared to the coating over the same stainless steel without any nitriding pre-treatment. It is a fact that a better adhesion is obtained in the duplex samples, and there is also a better matching of the thermal coefficients and the mechanical properties of the nitrided layer with the DLC coating, allowing in some way that the nitrided layer delayed the thermal degradation of the coating deposited over it.

In this paper, it is shown that the adhesion and the hardness are related and that can be evaluated from a heat treatment. This is a new result, which the authors can speculate as being of much importance to any measure of nanohardness in thin films.

Further studies are necessary to relate the coatings structure to the properties of the interface with the nitrided substrate and the early stages of growing, and their behaviour at different temperatures.

Conflicts of interest

The authors declare no conflicts of interest.

Acknowledgements

The authors would like to thank students of the Surface Engineering Group (UTN) for their collaboration in the experimental tasks. Also to Dipl. Eng. Federico Lasserre at that time at Saarland University (Germany), for the help in SEM and WLI experiments.PID UTI 4716 TC UTN, 2018-2021. SUMA2 Network, EU FP7-PEOPLE-2012-IRSES, Project Nr. 318903

REFERENCES

[1] Choy K. Chemical vapour deposition of coatings. Prog Mater Sci 2003;48:57–170.
[2] Robertson J. Diamond-like amorphous carbon. Mater Sci Eng R Rep 2002;37:129–281.
[3] Trava-Airoldi VJ, Bonetti LF, Capote G, Santos LV, Corat EJ. A comparison of DLC film properties obtained by r.f. PACVD, IBAD, and enhanced pulsed-DC PACVD. Surf Coat Technol 2007;202:549–54.
[4] Chicot D, Puchi-Cabrera ES, Decoopman X, Roudet F, Lesage J, Staia MH. Diamond-like carbon film deposited on nitrided 316L stainless steel substrate: a hardness depth-profile modeling. Diam Relat Mater 2011;20:1344–52.
[5] Snyders R, Bousser E, Amireault P, Klemberg-Sapieha JE, Park E, Taylor K, et al. Tribo-mechanical properties of DLC

coatings deposited on nitrided biomedical stainless steel. Plasma Process Polym 2007;4:S640–6.
[6] Azzi M, Paquette M, Szpunar JA, Klemberg-sapieha JE, Martinu L. Tribocorrosion behaviour of DLC-coated 316L stainless steel. Wear 2009;267:860–6.
[7] Shioga JPHT, Binder C, Hammes G, Klein AN, de Mello DB. Effects of different plasma nitrided layers on the tribological performance of DLC coatings. Mater Res 2016;19:1180–8.
[8] Kovaci H, Baran Ö, Yetim AF, Bozkurt YB, Kara L, Çelik A. The friction and wear performance of DLC coatings deposited on plasma nitrided AISI 4140 steel by magnetron sputtering under air and vacuum conditions. Surf Coat Technol 2018;349:969–79.
[9] Podgornik B, Vižintin J, Wänstrand O, Larsson M, Hogmark S, Ronkainen H, et al. Tribological properties of plasma nitrided and hard coated AISI 4140 steel. Wear 2001;249:254–9.
[10] Dalibon EL, Charadia R, Cabo A, Trava-Airoldi VJ, Brühl SP. Evaluation of the mechanical behaviour of a DLC film on plasma nitrided AISI 420 with different surface finishing. Surf Coat Technol 2013;235:735–40.
[11] Dalibon EL, Trava-Airoldi VJ, Pereira LA, Cabo A, Brühl SP. Wear resistance of nitrided and DLC coated PH stainless steel. Surf Coat Technol 2014;255:22–7.
[12] Forsich C, Heim D, Mueller T. Influence of the deposition temperature on mechanical and tribological properties of a-C:H:Si coatings on nitrided and postoxidized steel deposited by DC-PACVD. Surf Coat Technol 2008;203: 521–5.
[13] Kovaleva MG, Kolpakov AJ, Poplavsky AI, Galkina ME. Effect of vacuum annealing on tribological behavior of nanosized diamond like carbon coatings produced by pulse vacuum arc method. J Frict Wear 2013;34:481–6.
[14] Ito H, Yamamoto K, Masuko M. Thermal stability of UBM sputtered DLC coatings with various hydrogen contents. Thin Solid Films 2008;517:1115–9.
[15] Leng YX, Chen JY, Yang P, Sun H, Wan GJ, Huang N. Mechanical properties and thermomechanical stability of diamond-like carbon films synthesized by pulsed vacuum arc plasma deposition. Surf Coat Technol 2003;173:67–73.
[16] Choi J, Miyagawa S, Nakao S, Ikeyama M, Miyagawa Y. Thermal stability of diamond-like carbon films deposited by plasma based ion implantation technique with bipolar pulses. Diam Relat Mater 2006;15:948–51.
[17] Moolsradoo N, Abe S, Watanabe S. Thermal stability and tribological performance of DLC-Si-O films. Adv Mater Sci Eng 2011.
[18] Hatada R, Baba K, Flege S, Ensinger W. Long-term thermal stability of Si-containing diamond-like carbon fi lms prepared by plasma source ion implantation. Surf Coat Technol 2016;305:93–8.
[19] Dai W, Gao X, Liu J, Wang Q. Microstructure, mechanical property and thermal stability of diamond-like carbon coatings with Al, Cr and Si multi-doping. Diam Relat Mater 2016;70:98–104.
[20] Brühl SP, Dalibon EL, Ghafoor N, Rogström L, Trava-Airoldi VJ, Odén M. Carbon based coatings deposited on nitrided stainless steel: study of thermal degradation. In: Meyers M, et al., editors. Proc. 3rd Pan Am. Mater. Congress. The minerals, metals & materials series. Springer; 2017.
[21] Guitar A, Trava-airoldi VJ, Mu F, Brühl SP. Plasma nitriding and DLC coatings for corrosion protection of precipitation hardening stainless steel. Adv Eng Mater 2015;18:826–32.
[22] Zhang S, Lam X, Li X. Thermal stability and oxidation properties of magnetron sputtered diamond-like carbon and its nanocomposite coatings. Diam Relat Mater 2006;15:972–6.
[23] Casiraghi C, Ferrari AC, Robertson J. Raman spectroscopy of hydrogenated amorphous carbons. Phys Rev B 2005;72:1–13.
[24] Donnet C, Erdemir A. Tribology of diamond-like carbon films. fundamentals and applications. USA: Springer; 2008.
[25] Holmberg K, Matthews A. Coatings tribology properties, mechanisms, techniques and applications in surface engineering. UK: Elsevier; 2009.
[26] Wang L, Nie X, Hu X. Effect of thermal annealing on tribological and corrosion properties of DLC coatings. J Mater Eng Perform 2013;22:3093–100.
[27] Bayer RG. Wear analysis for engineers. New York: HNB Publishing; 2002.
[28] Peter S, Günther M, Gordan O, Berg S, Zahn DRT, Seyller T. Experimental analysis of the thermal annealing of hard a-C:H films. Diam Relat Mater 2014;45:43–57.
[29] Sheng R, Li L, Su D, Peng J, Gao J, Zhao K, et al. Effect of unbonded hydrogen on amorphous carbon film deposited by PECVD with annealing treatment. Diam Relat Mater 2018;81:146–53.
[30] Podgornik B, Vižintin J, Leskovšek V. Tribological properties of plasma and pulse plasma nitrided AISI 4140 steel. Surf Coat Technol 1998;108–109:454–60.
[31] Borges CFM, Pfender E, Heberlein J. Influence of nitrided and carbonitrided interlayers on enhanced nucleation of diamond on stainless steel 304. Diam Relat Mater 2001;10:1983–90.
[32] Li D, Guruvenket S, Azzi M, Szpunar JA, Klemberg-Sapieha JE, Martinu L. Corrosion and tribo-corrosion behavior of a-SiCx:H, a-SiNx:H and a-SiCxNy:H coatings on SS301 substrate. Surf Coat Technol 2010;204:1616–22.
[33] Chen CW, Huang CC, Lin YY, Chen LC, Chen KH. The affinity of Si—N and Si—C bonding in amorphous silicon carbon nitride (a-SiCN) thin film. Diam Relat Mater 2005;14:1126–30.
[34] Wei Ch, Yen JY. Effect of film thickness and interlayer on the adhesion strength of diamond like carbon films on different substrate. Diam Relat Mater 2007;16:1325–30.
[35] Li XY, Sun Y, Bell T. Stability of the nitrogen S-phase in austenitic stainless steel. Int J Mater Res 1999;90:901–7.
[36] Maheswaran R, Thiruvadigal DJ, Gopalakrishnan C. Thermal instability of DLC film surface morphology – an AFM study. AIP Conf Proc 2012;1447:789–90.
[37] Cloutier M, Harnagea C, Hale P, Seddiki O, Rosei F, Mantovani D. Long-term stability of hydrogenated DLC coatings: effects of aging on the structural, chemical and mechanical properties. Diam Relat Mater 2014;48:65–72.
[38] Li H, Xu T, Wang C, Chen J, Zhou H, Liu H. Annealing effect on the structure, mechanical and tribological properties of hydrogenated diamond-like carbon films. Thin Solid Films 2006;515:2153–60.